INTERPLAY OF ANISOTROPY OF MOMENTUM DISTRIBUTIONS AND MEAN FIELDS IN HEAVY-ION COLLISIONS

By

Christian Helmut Simon

A THESIS

Submitted to
Michigan State University
in partial fulfillment of the requirements
for the degree of

MASTER OF SCIENCE

Physics

2011

UMI Number: 1498446

All rights reserved

INFORMATION TO ALL USERS
The quality of this reproduction is dependent on the quality of the copy submitted.

In the unlikely event that the author did not send a complete manuscript
and there are missing pages, these will be noted. Also, if material had to be removed,
a note will indicate the deletion.

UMI 1498446

Copyright 2011 by ProQuest LLC.

All rights reserved. This edition of the work is protected against
unauthorized copying under Title 17, United States Code.

ProQuest LLC.
789 East Eisenhower Parkway
P.O. Box 1346
Ann Arbor, MI 48106 - 1346

ABSTRACT

INTERPLAY OF ANISOTROPY OF MOMENTUM DISTRIBUTIONS AND MEAN FIELDS IN HEAVY-ION COLLISIONS

By

Christian Helmut Simon

We construct an explicitly anisotropic nucleonic mean field, for a phase-space density anisotropic in momentum, convenient for modeling of nuclear reactions, using separable interactions in momentum space. We demonstrate the flexibility of our separable model for the potential energy density V associated with the momentum-dependent mean field U, by approximating the respective expressions by Welke *et al.* which also serve as reference. Therefore, we apply an expansion in spherical harmonics, comprising scalar and tensorial terms to Welke's potential energy density, laying open the anisotropy of the mean field. Ground-state properties in the reference model can be well described within our framework. The anisotropy in our model is parameterized by relying on anisotropic Gaussian distributions for excited-matter scenarios. We show that the strongly anisotropic mean field of 2 Fermi spheres in momentum space can be reproduced within our framework. As for the contribution to the velocity field deduced from our mean field parameterization, we find that for large anisotropies particle velocities tend to be weakly directed along the transverse momentum axis. Our parameterization can be applied in BUU transport simulations with gain over an approach of the type of Welke *et al.* in reduced computational cost and reduced error-proneness.

For the benefit of mankind.

ACKNOWLEDGMENTS

First of all, I would like to thank Prof. Dr. Pawel Danielewicz most sincerely for accepting me as his master's student, for his continuous support during the last twelve months and for providing me the opportunity to dip into Nuclear Theory. This thesis would not have been possible unless he had shown such an amount of patience confronted with the huge number of questions I put to him.

Moreover, I owe my deepest gratitude to the other members of my committee, Prof. Dr. Bill Lynch and Prof. Dr. Scott Pratt. I would especially like to thank them for suggestions for revising my thesis.

In addition, I am indebted to my colleagues in the Danielewicz group for supporting my work. I would like to show my gratitude to Jun Hong and Brent Barker. They have made available their support in a number of ways.

I also would like to thank Dr. Muslema Pervin and Dietrich Roscher for the wonderful office climate.

To conclude, it is a pleasure to thank my parents who made my physics study possible and encouraged me to study abroad at Michigan State University. In a remarkable way, they have always promoted my technical and physical interests.

TABLE OF CONTENTS

List of Figures . . . . . **vi**

1 Introduction **1**

2 Theory **4**
2.1 Momentum dependence of mean fields and implicit anisotropy 4
2.1.1 Mean field comparison between Gale *et al.* and Welke *et al.* models . 6
2.2 Separable interactions and anisotropic mean fields 9
2.2.1 Mean field for an anisotropic Gaussian distribution 12

3 Modeling **14**
3.1 Ground state in energy density and mean field 14
3.2 Energy density and mean field for excited nuclear matter 16
3.2.1 Isotropic Gaussian phase-space density 16
3.2.2 Anisotropic Gaussian phase-space density 19
3.3 Comparison of anisotropy for 2 Fermi spheres 25
3.4 Contribution to the velocity field due to an anisotropic mean field 26

4 Proposed organization of BUU transport simulations **29**

5 Conclusion **31**

Bibliography **35**

LIST OF FIGURES

Figure 2.1 Situation within the local rest frame of 2 Fermi spheres separated by $p_0 = 800\,\mathrm{MeV}$ in p-space. 6

Figure 2.2 Single particle potential as function of ϑ (cf. fig. 2.1) for different momentum magnitudes p. Dashed lines refer to GBD and solid lines to Welke *et al.*. 7

Figure 3.1 Optical potential U of the ground state as function of momentum p for Welke *et al.* and for the separable approach, at normal density. 14

Figure 3.2 Energy density V at zero temperature as function of density ρ for Welke *et al.* and the separable approach. 15

Figure 3.3 Optical potential U of an isotropic Gaussian as function of momentum p for Welke *et al.* and for the separable approach, at normal density. Results for different widths σ are visualized for the range dictated by achievable temperatures in the collisions. 17

Figure 3.4 Same as in fig. 3.3 but with two separable isotropic terms in the mean field parameterization. 18

Figure 3.5 Energy density V as function of σ/Λ for an isotropic Gaussian at $2\rho_0$ for Welke *et al.* and for the separable model. 19

Figure 3.6 Energy density V (3.9) as function of ε for an anisotropic Gaussian compared with Welke *et al.*, at $2\rho_0$. 21

Figure 3.7 Anisotropic mean field U (2.17) as function of $\cos(\vartheta)$ for $\varepsilon = 0.5$ and $\varepsilon = 1.5$ at a momentum magnitude of $p = 2p_\mathrm{F}^{(0)}$. The parameterization according to Welke *et al.* is compared to our separable one using $b = 1.15$ and $a = 1.15$. 23

Figure 3.8 Anisotropic mean field U (2.17) as function of $\cos(\vartheta)$ for $\varepsilon = 0.3$ at momentum magnitudes of $p = p_\mathrm{F}^{(0)}$ and $p = 2p_\mathrm{F}^{(0)}$. 23

Figure 3.9 Anisotropic mean field U (2.17) as function of $\cos(\vartheta)$ for $\varepsilon = 1.0$ at momentum magnitudes of $p = p_\mathrm{F}^{(0)}$ and $p = 2p_\mathrm{F}^{(0)}$. 24

Figure 3.10 Anisotropic mean field U (2.17) in the center of mass of 2 Fermi spheres separated by $p_0 = 800\,\mathrm{MeV}$ as function of $\cos(\vartheta)$ at a momentum magnitude of $p = p_\mathrm{F}^{(0)}$ 25

Figure 3.11 Contribution to the velocity field $\Delta\mathbf{v}$ associated with our mean field (2.17) for an isotropic Gaussian ($\varepsilon = 0$) in 2 dimensions. 27

Figure 3.12 Contribution to the velocity field $\Delta\mathbf{v}$ associated with our mean field (2.17) for an anisotropic Gaussian ($\varepsilon = 1.5$) in 2 dimensions. 28

Chapter 1

Introduction

In heavy-ion collision theory, the impact of the momentum dependence of the nucleon optical potential U on the deduced nuclear equation of state is of utmost importance. Not only does it play a significant role in generating collective flow according to calculations [Pan93], but it is also crucial for particle production like pions and kaons in transport simulations [Tei97]. In order to properly constrain the nuclear compression modulus K, defined as

$$K = p_{\mathrm{F}}^2 \frac{d^2(E/A)}{dp_{\mathrm{F}}^2}, \tag{1.1}$$

where p_{F} is the Fermi momentum and E/A the binding energy per nucleon, one also needs to take the momentum dependence of nucleon-nucleon interactions into account. In 1976, Blaizot et al. [Bla76] showed that K could be inferred by measuring the energy of the isoscalar monopole resonance in medium and heavy nuclei, and found a value of $K = 210 \pm 30\,\mathrm{MeV}$. Flow data, however, for a long time seemed to be describable by both a momentum-dependent "soft" eos ($K \approx 210\,\mathrm{MeV}$) or a momentum-independent "hard" eos ($K \approx 380\,\mathrm{MeV}$) [Aic87], [Gal87]. These findings can only be brought into accordance if one assumes nuclear matter to be "soft" and nuclear interactions to be dependent on p. In fact, Pan and Danielewicz [Pan93] confirmed this conclusion by obtaining the best agreement between sideward flow data and the results from transport calculations when applying a momentum-dependent "soft" eos.

Several approaches to the momentum dependence of the optical potential can be found in the

literature (see [Zha94] for a review article). The most prominent ones used in BUU [Ueh33] calculations are the early parameterization by Gogny [Gog75], the ansatz by Gale, Bertsch and Das Gupta [Gal87] and the one by Welke *et al.* [Wel88]. In chapter 2, the latter ones are introduced in more detail, and Welke results will serve as reference for our calculations. Following Landau theory [Noz99], these approaches comprise a functional expression for the potential energy density V and its functional derivative with respect to the single-particle phase-space density $f(\mathbf{r}, \mathbf{p})$,

$$U = \left. \frac{\delta V}{\delta f} \right|_{\mathbf{p}}, \tag{1.2}$$

namely the nucleonic mean field (or optical potential) U.

If the density f is anisotropic in momentum space, one would expect by symmetry the mean field to also exhibit an anisotropic behavior explicitly. Parameterizing f by some anisotropy parameter ε can be useful in discussing partially equilibrated scenarios in momentum space, developing after the original nucleons from the Fermi spheres depicting target and projectile had a chance to collide with the nucleons from the counterpart nucleus. Thus, the idea of making the mean field U itself anisotropic for an anisotropic scenario has great appeal to us, especially since some of the models employed in practice lack this feature.

This thesis is devoted to deriving a parameterization for the energy density V and the optical potential U in heavy-ion collisions for anisotropic systems that can be efficiently used in BUU calculations, particularly in the code by Danielewicz [Dan00]. It involves introducing separable interactions in p-space in terms of an expansion in spherical harmonics through which anisotropy explicitly enters the mean field. Since Welke's approach requires the determination of a 3-dimensional integral for every relevant phase-space location at every time step (see chapter 2), it is – in general – computationally very costly [Tei97]. In chapter 2,

we present the models by Gale, Bertsch, Das Gupta (GBD) and by Welke before developing our own ansatz for V and U. Chapter 3 consists of the detailed derivation of an anisotropic mean field, cross-checking our results against Welke's parameterization for the nuclear ground state and excited matter. The benefits of our new model for BUU calculations in terms of increased computational efficiency and reduced error-proneness, which are disadvantages of Welke's model, are outlined in chapter 4. Chapter 5 is used to summarize and draw conclusions.

Chapter 2

Theory

2.1 Momentum dependence of mean fields and implicit anisotropy

The parameterizations by GBD and by Welke are presented in this section. We first discuss the mathematical framework used for the potential energy density V and the mean field U. In an appended subsection, we exemplify the differences between these models by considering an anisotropic mean field scenario.

At first appearance, the above two parameterizations look quite similar. Their special distinguishing mark is the local momentum average $\langle \mathbf{p} \rangle$ implemented in GBD (2.1) in contrast to Welke's convolution with the phase-space density f (2.3). Both models are based on Skyrme-type interactions [Sky59] for the density-dependent part of the energy density and the mean field. In the case of GBD, the potential energy density can be written as

$$\begin{aligned} V_{\mathrm{GBD}}(\rho(\mathbf{r})) = & \frac{A}{2}\frac{\rho^2(\mathbf{r})}{\rho_0} + \frac{B}{\sigma+1}\frac{\rho^{\sigma+1}(\mathbf{r})}{\rho_0^{\sigma}} \\ & + \frac{C\rho(\mathbf{r})}{\rho_0}\int d^3p' \frac{f(\mathbf{r},\mathbf{p}')}{1+\left[\frac{\mathbf{p}'-\langle\mathbf{p}\rangle}{\Lambda}\right]^2}. \end{aligned} \tag{2.1}$$

Accordingly, one obtains the mean field

$$\begin{aligned} U_{\mathrm{GBD}}(\rho(\mathbf{r}),\mathbf{p}) = \; & A\left(\frac{\rho(\mathbf{r})}{\rho_0}\right) + B\left(\frac{\rho(\mathbf{r})}{\rho_0}\right)^{\sigma} \\ & + \frac{C}{\rho_0}\int d^3p' \frac{f(\mathbf{r},\mathbf{p}')}{1+\left[\frac{\mathbf{p}'-\langle\mathbf{p}\rangle}{\Lambda}\right]^2} \\ & + \frac{C}{\rho_0}\frac{\rho(\mathbf{r})}{1+\left[\frac{\mathbf{p}-\langle\mathbf{p}\rangle}{\Lambda}\right]^2}. \end{aligned} \tag{2.2}$$

Note that f – where not otherwise stated – represents the phase-space density of the single particle which is normalized according to $\rho(\mathbf{r}) = \int d^3p' f(\mathbf{r},\mathbf{p}')$.

Following Welke, the energy density is parameterized as

$$\begin{aligned} V_{\mathrm{Welke}}(\rho(\mathbf{r})) = \; & \frac{A}{2}\frac{\rho^2(\mathbf{r})}{\rho_0} + \frac{B}{\sigma+1}\frac{\rho^{\sigma+1}(\mathbf{r})}{\rho_0^{\sigma}} \\ & + \frac{C}{\rho_0}\int\int d^3p\, d^3p' \frac{f(\mathbf{r},\mathbf{p})f(\mathbf{r},\mathbf{p}')}{1+\left[\frac{\mathbf{p}-\mathbf{p}'}{\Lambda}\right]^2}. \end{aligned} \tag{2.3}$$

This leads to a mean field of the form

$$\begin{aligned} U_{\mathrm{Welke}}(\rho(\mathbf{r}),\mathbf{p}) = \; & A\left(\frac{\rho(\mathbf{r})}{\rho_0}\right) + B\left(\frac{\rho(\mathbf{r})}{\rho_0}\right)^{\sigma} \\ & + 2\frac{C}{\rho_0}\int d^3p' \frac{f(\mathbf{r},\mathbf{p}')}{1+\left[\frac{\mathbf{p}-\mathbf{p}'}{\Lambda}\right]^2}. \end{aligned} \tag{2.4}$$

An inherent part of both models are the 5 parameters A, B, σ, C and Λ. They are determined by requiring a binding energy per nucleon of $E/A = -16\,\mathrm{MeV}$ at saturation density $\rho_0 = 0.16\,\mathrm{fm}^{-3}$, $K \simeq 215\,\mathrm{MeV}$, $U(\rho_0, p=0) \simeq -75\,\mathrm{MeV}$ and $U(\rho_0, p^2/2m \simeq 300\,\mathrm{MeV}) = 0$.

In the following, we present an anisotropic scenario in momentum space in order to visually compare GBD with Welke.

2.1.1 Mean field comparison between Gale *et al.* and Welke *et al.* models

Of relevance to our considerations in chapter 3 is the following particular scenario for which U_{GBD} is compared with U_{Welke}. In [Wel88], Welke *et al.* examined (2.2) and (2.4) in the local rest frame of two cold Fermi spheres

$$f(\mathbf{p}) = \frac{g}{(2\pi\hbar)^3}\theta(p_{\mathrm{F}} - |\mathbf{p} \mp \mathbf{p}_0/2|), \tag{2.5}$$

separated by $p_0 = 800\,\mathrm{MeV}$ in momentum space. The scenario is sketched in fig. 2.1.

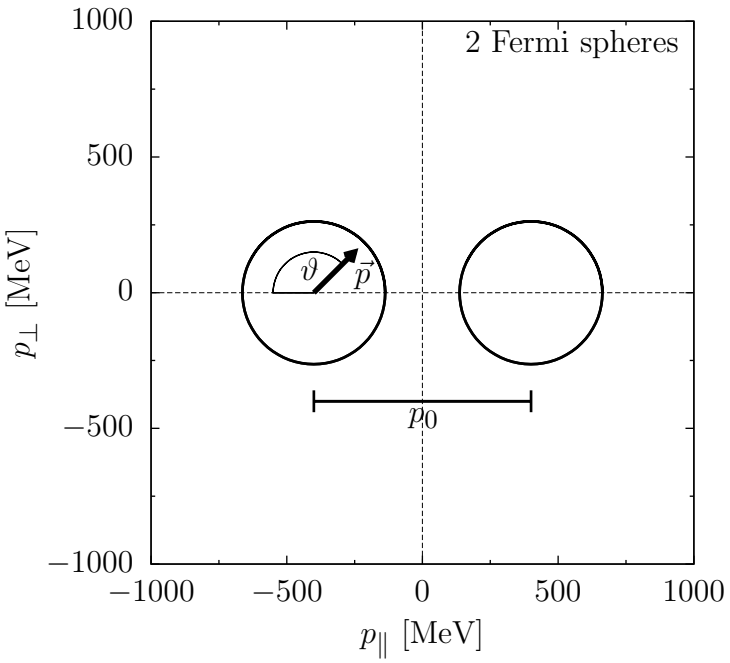

Figure 2.1: Situation within the local rest frame of 2 Fermi spheres separated by $p_0 = 800\,\mathrm{MeV}$ in p-space.

The single-particle potentials (cf. fig. 2.2) associated with this scenario are plotted as functions of the polar angle ϑ (defined in fig. 2.1) for different momenta. For fig. 2.2, we use a

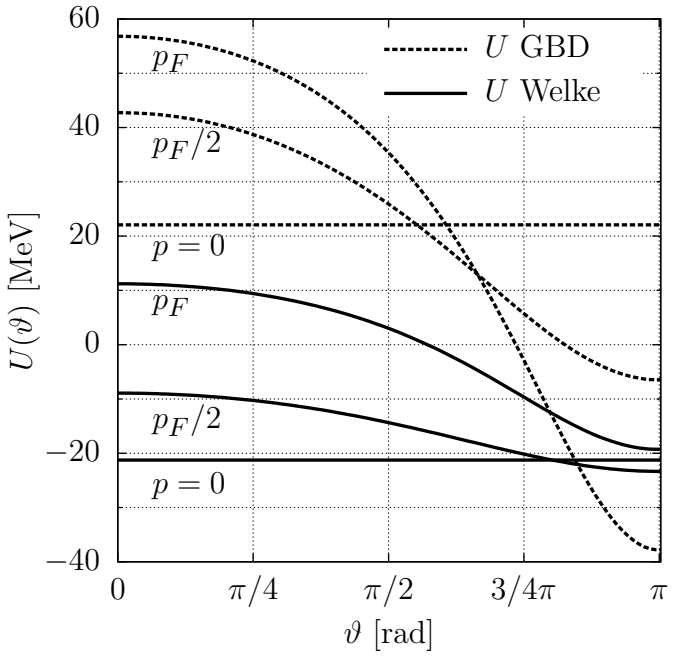

Figure 2.2: Single particle potential as function of ϑ (cf. fig. 2.1) for different momentum magnitudes p. Dashed lines refer to GBD and solid lines to Welke *et al.*.

vector $\mathbf{p}$ relative to the center of one sphere, with the angle about that center. The mean fields vary not only in overall offset but also in dependence on angle.

As to the 5 parameters A, B, σ, C and Λ, one uses $A = -144.9\,\mathrm{MeV}$, $B = 203.3\,\mathrm{MeV}$, $\sigma = 7/6$, $C = -75\,\mathrm{MeV}$ and $\Lambda = 1.5\,p_\mathrm{F}^{(0)}$ in the GBD model [Gal87]. For Welke's parameterization, the parameter values of $A = -110.44\,\mathrm{MeV}$, $B = 140.9\,\mathrm{MeV}$, $\sigma = 1.24$, $C = -64.95\,\mathrm{MeV}$ and $\Lambda = 1.58\,p_\mathrm{F}^{(0)}$ are employed [Wel88]. The parameters are chosen to meet the requirements mentioned in § 2.1. The Fermi momentum $p_\mathrm{F}^{(0)} \approx 263\,\mathrm{MeV}$ of cold nuclear matter, with a degeneracy $g = 4$ (protons and neutrons are not treated separately), is referred to in both cases.

When dealing with Fermi spheres in GBD or Welke one can find analytical solutions to the integrals with a Yukawa-type interaction kernel appearing in (2.1) - (2.4). Thus, one can circumvent running computationally costly integration routines, although it does not help in

carrying out collision simulations, since distributions quickly depart from the Fermi spheres. Whenever we deal with ground-state properties in this thesis we make use of one of the following expressions taken from [Wel88], and also confirmed by the present author:

$$\int_0^{p_\mathrm{F}}\int_0^{p_\mathrm{F}} d^3p\, d^3p' \frac{1}{1+\left[\frac{\mathbf{p}-\mathbf{p}'}{\Lambda}\right]^2} = \frac{32\pi^2}{3}p_\mathrm{F}^4\Lambda^2\Bigg[\ \frac{3}{8} - \frac{\Lambda}{2p_\mathrm{F}}\arctan\frac{2p_\mathrm{F}}{\Lambda} - \frac{\Lambda^2}{16p_\mathrm{F}^2} + \left(\frac{3}{16}\frac{\Lambda^2}{p_\mathrm{F}^2} + \frac{1}{64}\frac{\Lambda^4}{p_\mathrm{F}^4}\right)\ln\left(1+\frac{4p_\mathrm{F}^2}{\Lambda^2}\right)\Bigg], \quad (2.6)$$

$$\int_0^{p_\mathrm{F}} d^3p' \frac{1}{1+\left[\frac{\mathbf{p}-\mathbf{p}'}{\Lambda}\right]^2} = \pi\Lambda^3\Bigg[\ \frac{p_\mathrm{F}^2+\Lambda^2-p^2}{2p\Lambda}\ln\frac{(p+p_\mathrm{F})^2+\Lambda^2}{(p-p_\mathrm{F})^2+\Lambda^2} + \frac{2p_\mathrm{F}}{\Lambda} - 2\left(\arctan\frac{p+p_\mathrm{F}}{\Lambda} - \arctan\frac{p-p_\mathrm{F}}{\Lambda}\right)\Bigg]. \quad (2.7)$$

In chapter 3, we compare our results for an explicitly anisotropic mean field to result of Welke *et al.*, when combining 2 Fermi spheres.

2.2 Separable interactions and anisotropic mean fields

This section is devoted to outlining our model for the momentum dependence of the potential energy density V and the optical potential U. We show how to parameterize a separable approach for interactions in p-space and how to make the mean field explicitly anisotropic for anisotropic f.

Guidance for our model is provided by the manipulation applied to the momentum-dependent term by Welke *et al.*. However, as will become clear in chapters 3 and 4, our approach stands on its own feet; Welke results are used during the modeling process as a point of orientation, not as an auxiliary engine from which our model cannot be decoupled. We do not modify the form of the $\rho(\mathbf{r})$-dependent part and in fact, even assume the same values for the Skyrme parameters. In order to circumvent the convolution, which is inherent in the folding approach, we introduce separable interactions (2.8). This separation consists in representing the potential energy as a sum of products of single-particle terms, but both scalar and tensorial in nature:

$$\begin{aligned} V_{\text{sepint}}(\rho(\mathbf{r})) = \; & \frac{A}{2}\frac{\rho^2(\mathbf{r})}{\rho_0} + \frac{B}{\sigma+1}\frac{\rho^{\sigma+1}(\mathbf{r})}{\rho_0^{\sigma}} \\ & + \frac{C}{\rho_0}\Bigg[\int d^3p' \frac{f(\mathbf{r},\mathbf{p}')}{1+\left[\frac{\mathbf{p}'}{b\Lambda}\right]^2} \int d^3p' \frac{f(\mathbf{r},\mathbf{p}')}{1+\left[\frac{\mathbf{p}'}{b\Lambda}\right]^2} \\ & + \sum_{\alpha,\beta} T^{\alpha\beta}(\mathbf{r}) T^{\alpha\beta}(\mathbf{r}) \Bigg]. \end{aligned} \tag{2.8}$$

Within the center of mass of the system, the first prominent tensorial term, beyond the scalar, is likely to be quadrupole. To demonstrate the robustness of such a representation we will attempt to show that the results from the folding model of Welke *et al.* can be

well approximated within our separable model, including the reproduction of anisotropies of U. For simplicity, we take both the scalar and the tensor term as symmetric in the single-particle quantities. This is different from the GBD parameterization, scalar in our terminology. However, we take the form of the single-particle factor to be the same as in GBD [Gal87]. In the above, $T^{\alpha\beta}$ is a second rank Cartesian tensor [App89],[Dan05]:

$$T^{\alpha\beta}(\mathbf{r}) \equiv \int d^3p' c(\mathbf{p}') f(\mathbf{r}, \mathbf{p}')(p'^{\alpha} p'^{\beta} - \frac{1}{3} p'^2 \delta^{\alpha\beta}). \tag{2.9}$$

An important feature is its tracelessness,

$$T^{xx} + T^{yy} + T^{zz} = 0. \tag{2.10}$$

The function $c(\mathbf{p})$ in (2.9) is at this stage arbitrary and we will restrict its form in chapter 3. Note the dimensionless parameter b in the denominator of the scalar part (2.8).

According to (1.2), the optical potential is found by taking the functional derivative of (2.8) with respect to f. Due to the directionality involved and approximate axial symmetry of the phase-space density in heavy-ion collisions, the off-diagonal elements of (2.9) vanish reducing the summation over α, β to diagonal elements only. Here the tracelessness (2.10) of the tensor comes into play allowing us to express all elements in terms of T^{zz}. Upon taking

a functional derivative of (2.8), we get

$$\begin{aligned} U_{\text{sepint}}(\rho(\mathbf{r}),\mathbf{p}) = \; & A\left(\frac{\rho(\mathbf{r})}{\rho_0}\right) + B\left(\frac{\rho(\mathbf{r})}{\rho_0}\right)^{\sigma} \\ & + \frac{C}{\rho_0}\Bigg[\frac{2}{1+\left[\frac{p}{b\Lambda}\right]^2}\int d^3p' \frac{f(\mathbf{r},\mathbf{p}')}{1+\left[\frac{\mathbf{p}'}{b\Lambda}\right]^2} \\ & + 2c(p)\sum_{\alpha,\beta}(p^\alpha p^\beta - \frac{1}{3}p^2\delta^{\alpha\beta})T^{\alpha\beta}(\mathbf{r})\Bigg]. \end{aligned} \tag{2.11}$$

By transforming to spherical coordinates

$$\begin{aligned} p_x =& p\sin(\vartheta)\cos(\phi) \\ p_y =& p\sin(\vartheta)\sin(\phi) \\ p_z =& p\cos(\vartheta), \end{aligned} \tag{2.12}$$

and recalling the definition of $Y_{20}(\vartheta)$,

$$Y_{20}(\vartheta) = \sqrt{\frac{5}{16\pi}}\left(3\cos^2(\vartheta)-1\right), \tag{2.13}$$

one arrives at the following expression for the tensor contribution to the mean field:

$$\begin{aligned} & 2c(p)\sum_{\alpha,\beta}(p^\alpha p^\beta - \frac{1}{3}p^2\delta^{\alpha\beta})T^{\alpha\beta}(\mathbf{r}) \\ &= 2c(p)\left[-\frac{1}{2}(p^x)^2 - \frac{1}{2}(p^y)^2 + (p^z)^2\right]T^{zz}(\mathbf{r}) \\ &= c(p)p^2\left[3\cos^2(\vartheta)-1\right]T^{zz}(\mathbf{r}) \\ &= \sqrt{\frac{16\pi}{5}}c(p)p^2Y_{20}(\vartheta)T^{zz}(\mathbf{r}). \end{aligned} \tag{2.14}$$

Therewith, the optical potential (2.11) depends on anisotropy explicitly. The decisive term (2.14) vanishes for isotropic f since T^{zz} is zero for such cases by construction. Accordingly, we have introduced our framework for dealing with anisotropies in the phase-space density. For the parameterization of the isotropic part of (2.8) and (2.11), we mimic Welke's ground-state properties in chapter 3. The anisotropic part in (2.11) is modelled by using an anisotropic Gaussian described in the following subsection.

2.2.1 Mean field for an anisotropic Gaussian distribution

In order to arrive at an appropriate $c(p)$ for (2.11), we consider a single-particle phase-space density in the form of an anisotropic Gaussian. Gaussian momentum distributions allow for a level of generality in the vicinity of equilibrium. Because of folding in energy density, greater details than in a Gaussian may, in fact, have limited impact on the results. The anisotropy enters f through a parameter ε. For simplicity, in order to keep the volume in p-space occupied by the Gaussian constant, we scale the beam axis $p_\parallel$ and the perpendicular axis $p_\perp$ elliptically. Since a deformation of the phase-space density along the beam axis is a common scenario in heavy-ion collisions, ε is chosen such that a positive value is associated with a broadening in $p_\parallel$:

$$f_\varepsilon(\mathbf{r},\mathbf{p}) = \frac{\rho(\mathbf{r})}{(2\pi\sigma^2)^{3/2}} \exp\left[-\frac{1}{2\sigma^2}\left(p_\perp^2(1+\varepsilon) + \frac{p_\parallel^2}{(1+\varepsilon)^2}\right)\right]. \tag{2.15}$$

In order to make the optical potential linear in anisotropy for small ε, we expand the Gaussian phase-space density (2.15) about $\varepsilon = 0$ up to first order

$$f_\varepsilon(\mathbf{r},\mathbf{p}) \approx f_0(\mathbf{r},p)\left[1 + \varepsilon\sqrt{\frac{16\pi}{5}}\frac{p^2}{2\sigma^2}Y_{20}(\vartheta)\right], \tag{2.16}$$

and use this expansion in (2.11). We arrive at an ε-dependent expression for the mean field $U(\rho(\mathbf{r}), \mathbf{p})$ which only contains two one-dimensional, $\mathbf{p}$-independent integrals. The implications of this reduction of computational cost for BUU simulations are outlined in chapter 4. Upon inserting f of (2.16) into (2.11), we get

$$\begin{aligned} U_{\text{sepint}}(\rho(\mathbf{r}), \mathbf{p}) = \; & A\left(\frac{\rho(\mathbf{r})}{\rho_0}\right) + B\left(\frac{\rho(\mathbf{r})}{\rho_0}\right)^{\sigma} \\ & + C\frac{\rho(\mathbf{r})}{\rho_0}\Bigg[\frac{2}{1+\left[\frac{p}{b\Lambda}\right]^2}\frac{1}{\sigma^2}\int_0^\infty d\,p'\,\frac{2}{\sqrt{2\pi\sigma^2}}\frac{p'^2\exp[-\frac{p'^2}{2\sigma^2}]}{1+\left[\frac{p'}{b\Lambda}\right]^2} \\ & + \varepsilon\sqrt{\frac{16\pi}{5}}\frac{2}{15\sigma^4}c(p)p^2Y_{20}(\vartheta)\int_0^\infty d\,p'\,\frac{2}{\sqrt{2\pi\sigma^2}}p'^6c(p')\exp\left[-\frac{p'^2}{2\sigma^2}\right]\Bigg]. \end{aligned} \tag{2.17}$$

In the following chapter, we show how to construct V_{sepint} and U_{sepint} consistent with Welke's mean field. Therefore, one needs to find optimal values for the parameter b in (2.8) and (2.11) as well as an appropriate function $c(\mathbf{p})$.

Chapter 3

Modeling

3.1 Ground state in energy density and mean field

Within our considerations, our model mean field has right now two adjustable quantities: the parameter b and the function $c(\mathbf{p})$. Since it is essential to reproduce reasonably the features of the (isotropic) ground state of nuclear matter in our framework, and as done before by Welke, before proceeding with excited medium, we start the process of modeling by considering V_{sepint} and U_{sepint} for a single Fermi sphere in this section.

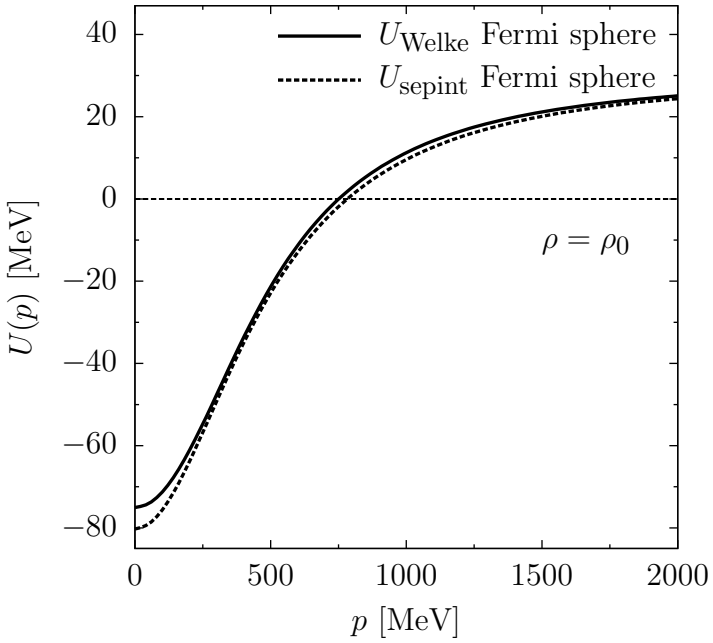

Figure 3.1: Optical potential U of the ground state as function of momentum p for Welke *et al.* and for the separable approach, at normal density.

The remarkable agreement between the two approaches and seen in fig. 3.1 and fig. 3.2 is found for $b = 1.16$. The energy density V_{sepint} proves to be more sensitive to variations in b in terms of increasing deviations between Welke and the separable model than the mean field. Presumably, this is due to the quadratic shape of the isotropic term in (2.8). The separable mean field agrees with Welke fairly well in the range $1.1 \leq b \leq 1.2$, also for higher densities than ρ_0. In fig. 3.2, one can see that the deviations between Welke and our model become larger for high densities but are still reasonable up to $4\rho_0$, given that the phenomenological approach by Welke *et al.* is a useful common-sense consideration, but not the truth.

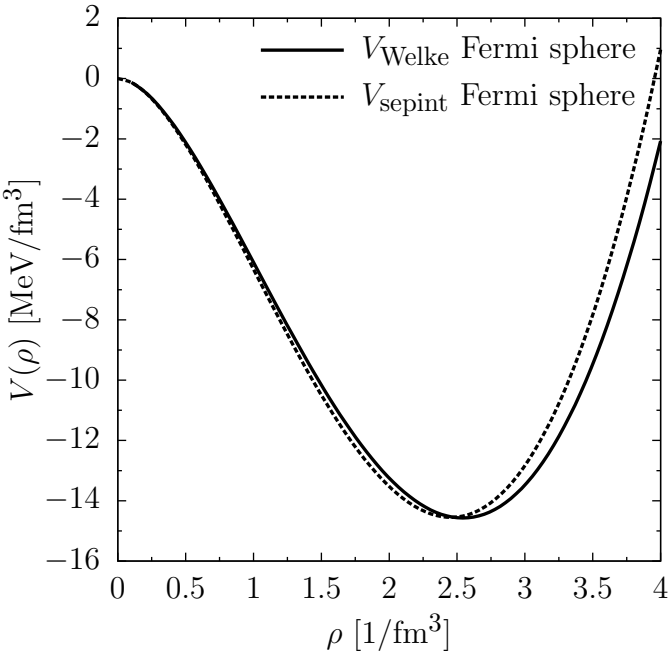

Figure 3.2: Energy density V at zero temperature as function of density ρ for Welke *et al.* and the separable approach.

As for zero temperature, Welke's convolutional model seems to be replacable by a separable ansatz. We now look at the behavior of our model in excited scenarios characterized by a schematic Gaussian phase-space density.

3.2 Energy density and mean field for excited nuclear matter

When considering excited states in momentum space, i.e. projectile and target start overlapping, the phase-space density f can be schematically represented by a Gaussian. This Gaussian distribution exhibits various degrees of anisotropy. Ultimately, we are interested in modeling strongly anisotropic scenarios within our separable framework. Such a situation occurs in the 2-Fermi-sphere system introduced in § 2.1.1. In order to arrive at this point, we firstly apply the parameterization which we found for cold nuclear matter to an isotropic Gaussian distribution (cf. § 3.2.1), and secondly constrain the anisotropic part of our mean field with anisotropic Gaussians (cf. § 3.2.2).

3.2.1 Isotropic Gaussian phase-space density

In order to establish a connection between a spherical distribution and an isotropic Gaussian density, we consider the density of kinetic energy

$$\left\langle \frac{p^2}{2m} \right\rangle = \int d^3p' \frac{p'^2}{2m} f(\mathbf{r}, \mathbf{p}'). \tag{3.1}$$

For a Fermi sphere, we find it to be

$$\left\langle \frac{p^2}{2m} \right\rangle = \frac{3}{5} \frac{p_{\mathrm{F}}^2}{2m} \rho. \tag{3.2}$$

An isotropic Gaussian yields

$$\left\langle \frac{p^2}{2m} \right\rangle = 3 \frac{\sigma^2}{2m} \rho. \tag{3.3}$$

Thus, we expect the Gaussian distribution to mimic cold nuclear matter if

$$\sigma = \frac{p_\mathrm{F}}{\sqrt{5}} = \frac{p_\mathrm{F}^{(0)} \sqrt[3]{\rho/\rho_0}}{\sqrt{5}}. \tag{3.4}$$

In the Boltzmann model, σ and T are connected via

$$\sigma^2 = m_\mathrm{N} T, \tag{3.5}$$

where m_N is the nucleon mass. Temperatures between $15\,\mathrm{MeV} \leq T \leq 170\,\mathrm{MeV}$ are of interest in heavy-ion collisions. With (3.4) and (3.5) we have a recipe how to appropriately use the Gaussian distribution in our separable model. At first, we consider the optical potential for a Gaussian at normal density.

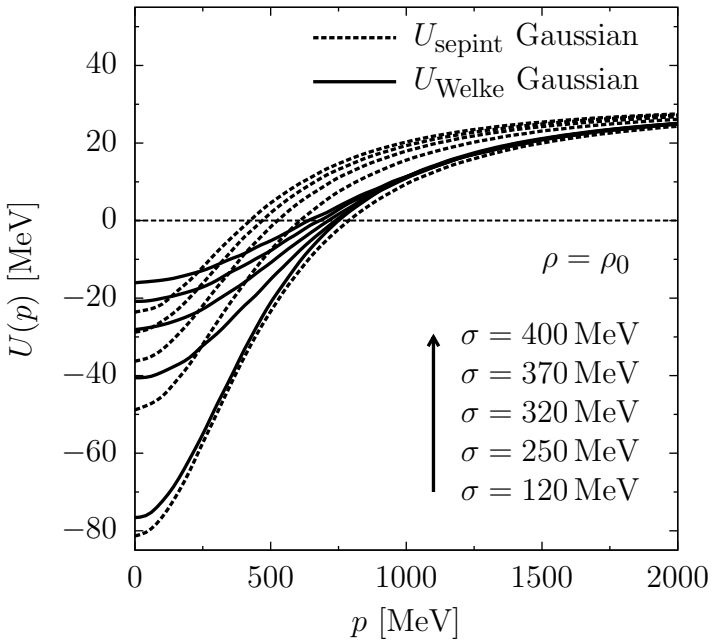

Figure 3.3: Optical potential U of an isotropic Gaussian as function of momentum p for Welke *et al.* and for the separable approach, at normal density. Results for different widths σ are visualized for the range dictated by achievable temperatures in the collisions.

We find a good agreement for $\sigma = 120\,\mathrm{MeV}$ which satisfies (3.4). For higher σ, i.e. higher temperatures up to 170 MeV (equivalent $\sigma = 400\,\mathrm{MeV}$), Welke's array of curves saturates for lower momenta than the separable one. This issue can be resolved by adding another separable isotropic term of the same kind that is already included in (2.11) to the mean field. For illustration, we added such a term, using $b = 1.1$ in the first term (weighted with 1.8), and $b = 4.0$ in the new second term (weighted with 0.1) to deal with high values of σ.

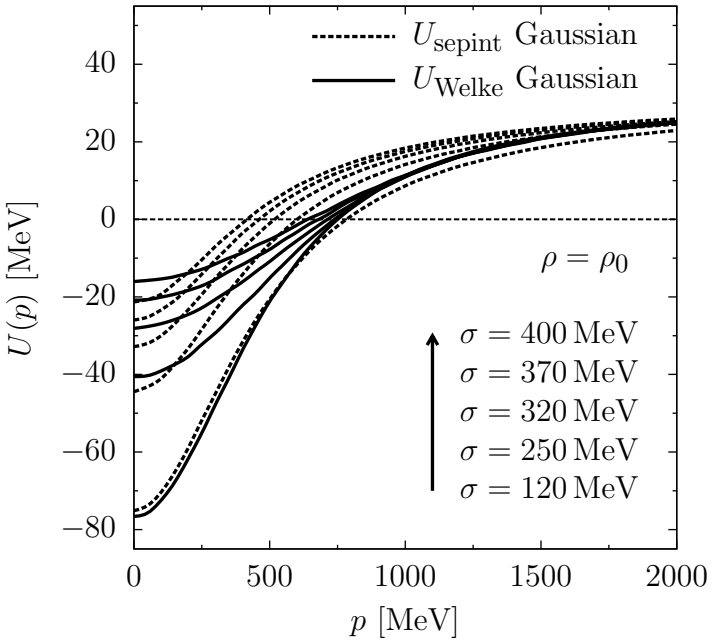

Figure 3.4: Same as in fig. 3.3 but with two separable isotropic terms in the mean field parameterization.

There is a marginal difference between fig. 3.3 and fig. 3.4, namely reduced deviations for high momenta in fig. 3.4 at the cost of an excellent agreement for the width mimicing cold nuclear matter. We simply intended to demonstrate that our separable approach can be enhanced when more terms are added. For higher densities ρ, the results do not significantly change.

In equilibrated Gaussian scenarios, the density to consider is $\rho = 2\rho_0$ accounting for the

matter from the two original nuclei overlapping. Thus, we will keep the density fixed at this value throughout the rest of this section. Apart from the optical potential U we are also interested in the energy density V for a Gaussian distribution. We consider V as a function of σ/Λ for $2\rho_0$ (cf. fig. 3.5), i.e. the starting width, mimicing the ground state, amounts to 150 MeV. The agreement is reasonable. For high temperatures, a deviation emerges that again can presumably be reduced when adding more terms to the separable expansion.

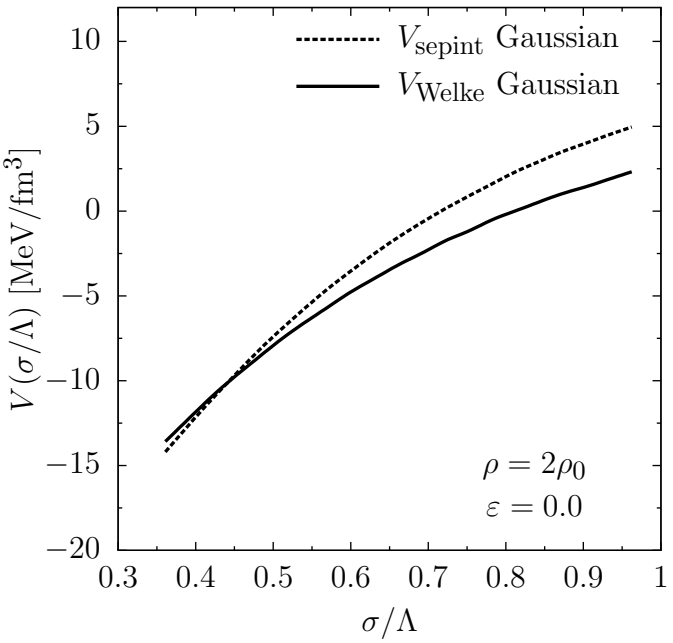

Figure 3.5: Energy density V as function of σ/Λ for an isotropic Gaussian at $2\rho_0$ for Welke *et al.* and for the separable model.

After showing that the Gaussian distribution works fine with $b = 1.16$ from cold nuclear matter we consider an anisotropic Gaussian scenario.

3.2.2 Anisotropic Gaussian phase-space density

In the framework of our model, the anisotropy of the phase-space density is described by the parameter ε which scales the width of the Gaussian distribution differently for the beam

axis and the perpendicular axes. One needs to relate this parameter to other, e.g. such as temperature, in order to determine the range in ε one should consider. We go back to eq. (3.1) to advance in our considerations. For an anisotropic Gaussian (2.15), one obtains

$$\left\langle \frac{p^2}{2m} \right\rangle = 3\frac{\sigma^2}{2m}\left[\frac{2}{(1+\varepsilon)} + (1+\varepsilon)^2\right]\rho. \tag{3.6}$$

We require that the quantity

$$\sigma_\varepsilon := \sigma\sqrt{\frac{2}{(1+\varepsilon)} + (1+\varepsilon)^2} \tag{3.7}$$

does not exceed the temperature bound of 170 MeV. The extremum is reached for $\varepsilon = -0.7$ and $\varepsilon = 1.5$. Other common sense considerations can be carried out that yield comparable values.

The function $c(p)$ is adjusted in the anisotropic part of the mean field U, rather than in the tensorial part of the potential energy density V. The reason is that by construction, given that the typical directionalities in collision scenarios along the beam axis and the perpendicular axes hold for our anisotropic Gaussian, the tensorial part

$$\sum_{\alpha,\beta} T^{\alpha\beta}(\mathbf{r})T^{\alpha\beta}(\mathbf{r}) = \frac{3}{2}(T^{zz}(\mathbf{r}))^2 \propto \varepsilon^2 \tag{3.8}$$

is always of the same positive sign. This is true in general, given that $T^{\alpha\beta}$ is symmetric and may be diagonalized. Thus, one would assume $V(\varepsilon)$ to have a negative curvature, when the tensorial part is appropriately multiplied with the negative parameter C (2.8). As we show in fig. 3.6, this is clearly not the case. However, within the framework of our model, we are capable of reproducing Welke's potential energy density V as function of anisotropy ε for an

anisotropic Gaussian, when only taking the Skyrme parameterization for the $\rho(\mathbf{r})$-dependent part of V and the part scalar in momentum into account:

$$V_{\text{sepint}}(\rho(\mathbf{r})) = \frac{A}{2}\frac{\rho^2(\mathbf{r})}{\rho_0} + \frac{B}{\sigma+1}\frac{\rho^{\sigma+1}(\mathbf{r})}{\rho_0^\sigma} + \frac{C}{\rho_0}\int d^3p' \frac{f_\varepsilon(\mathbf{r},\mathbf{p}')}{1+\left[\frac{\mathbf{p}'}{b\Lambda}\right]^2}\int d^3p' \frac{f_\varepsilon(\mathbf{r},\mathbf{p}')}{1+\left[\frac{\mathbf{p}'}{b\Lambda}\right]^2}. \tag{3.9}$$

Note the index ε of f in (3.9), indicating that we use the full anisotropic Gaussian as given in (2.15), and not the first-order expansion about small ε (2.16). In fig. 3.6, the energy density (3.9) is compared to Welke as function of anisotropy, for $\rho = 2\rho_0$.

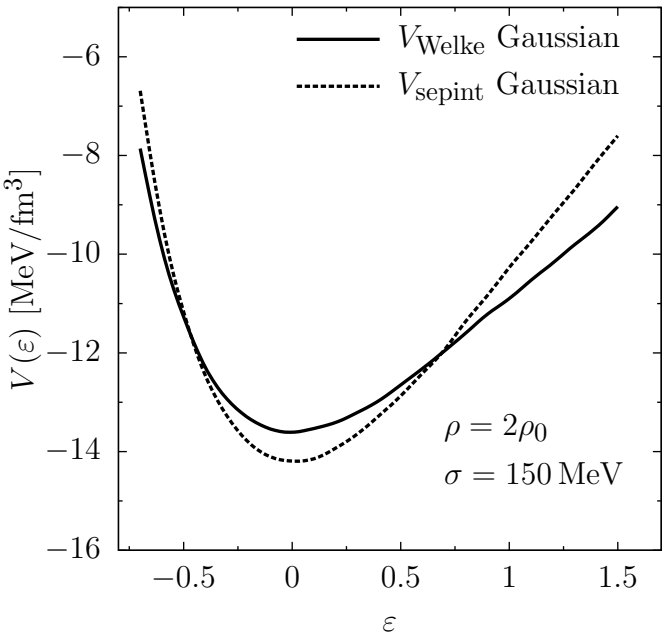

Figure 3.6: Energy density V (3.9) as function of ε for an anisotropic Gaussian compared with Welke *et al.*, at $2\rho_0$.

The good agreement indicates that the first part of our separable expansion (2.8), scalar in momentum, reasonably describes Welke in isotropic (cf. § 3.2.1) and anisotropic scenarios. Since $V(\varepsilon)$ does not qualify for restricting $c(p)$, we now turn to the anisotropic mean field

U. In the following adjustment of $c(p)$ through the mean field, we keep using a Gaussian phase-space density with a standard deviation of $\sigma = 150\,\mathrm{MeV}$ (cold matter equivalent for $2\rho_0$). The shape of U according to (2.17) is a simple parabola of the form

$$c_1(3x^2 - 1) + c_2 \tag{3.10}$$

with $x = \cos(\vartheta)$ as its argument as well as the curvature $3c_1$ and the vertex $c_2 - c_1$. Its vertex is parameterized by b, ε and $c(p)$ whereas its curvature depends on ε and also $c(p)$. We make the following ansatz for the function $c(p)$:

$$c(p) = \frac{1}{p^2 + (a\Lambda)^2}. \tag{3.11}$$

Although we are mostly interested in modeling strong anisotropies, we try to adjust the parameter a such that we have a good agreement for small, medium and big ε. Therefore, we consider the mean field U as function of $\cos(\vartheta)$ (cf. fig. 3.7) at a reasonably high momentum $p = 2p_{\mathrm{F}}^{(0)}$ for anisotropies of $\varepsilon = 0.5$ (medium) and $\varepsilon = 1.5$ (strong).

We find the best agreement for $b = 1.15$ – which we insignificantly changed from the original $b = 1.16$ – and $a = 1.15$. In addition, we apply these parameters to the anisotropic mean field for small $\varepsilon = 0.3$ (cf. fig. 3.8) and for $\varepsilon = 1.0$ (cf. fig. 3.9) right between 0.5 and 1.5. For $\varepsilon = 0.3$, the deviations between Welke and the separable approach are negligible, but the anisotropic behavior is also insignificant. Regarding $\varepsilon = 1.0$, we find a good agreement for the case of strong anisotropy ($p = 2p_{\mathrm{F}}^{(0)}$) and some deviation for $p = p_{\mathrm{F}}^{(0)}$.

Now we have acquired the tools to look at the 2-Fermi-sphere system described by Welke *et al.* with our separable model. This comparison is made in the next section.

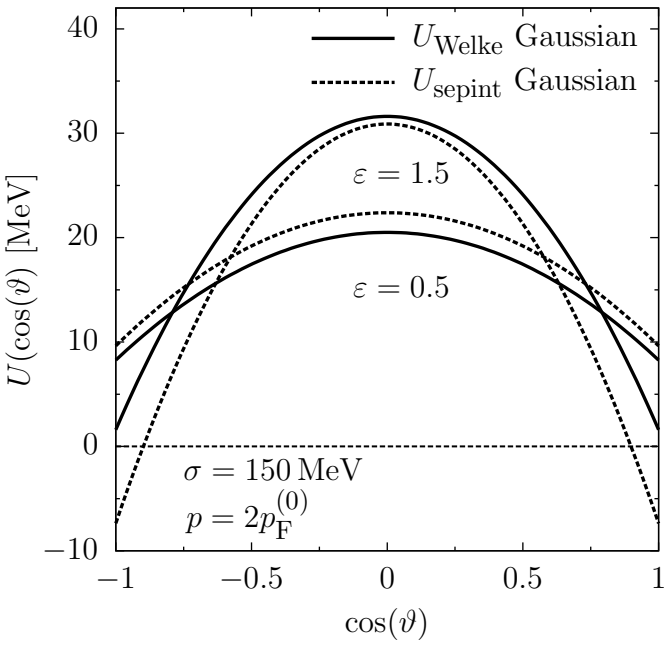

Figure 3.7: Anisotropic mean field U (2.17) as function of $\cos(\vartheta)$ for $\varepsilon = 0.5$ and $\varepsilon = 1.5$ at a momentum magnitude of $p = 2p_{\text{F}}^{(0)}$. The parameterization according to Welke *et al.* is compared to our separable one using $b = 1.15$ and $a = 1.15$.

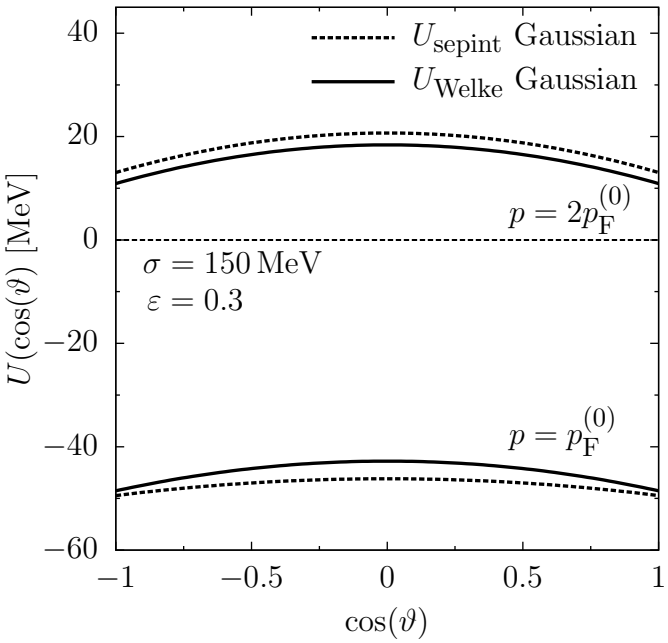

Figure 3.8: Anisotropic mean field U (2.17) as function of $\cos(\vartheta)$ for $\varepsilon = 0.3$ at momentum magnitudes of $p = p_{\text{F}}^{(0)}$ and $p = 2p_{\text{F}}^{(0)}$.

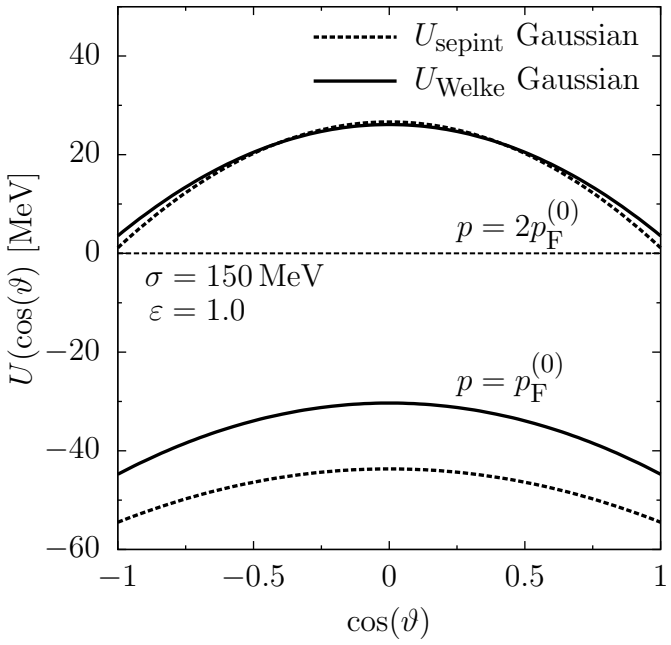

Figure 3.9: Anisotropic mean field U (2.17) as function of $\cos(\vartheta)$ for $\varepsilon = 1.0$ at momentum magnitudes of $p = p_{\text{F}}^{(0)}$ and $p = 2p_{\text{F}}^{(0)}$.

3.3 Comparison of anisotropy for 2 Fermi spheres

In § 2.1.1, we introduced a system consisting of 2 Fermi spheres separated by $p_0 = 800\,\mathrm{MeV}$ in momentum space (cf. fig. 2.1). Such a scenario is an ideal candidate to validate the separable anisotropic mean field we just derived since the anisotropy involved is remarkable, e.g. for a momentum of $p_\mathrm{F}^{(0)}$. In some contrast to what Welke *et al.* did, we consider a particle in the center of mass in p-space and define the angle ϑ with respect to the positive $p_\parallel$-axis.

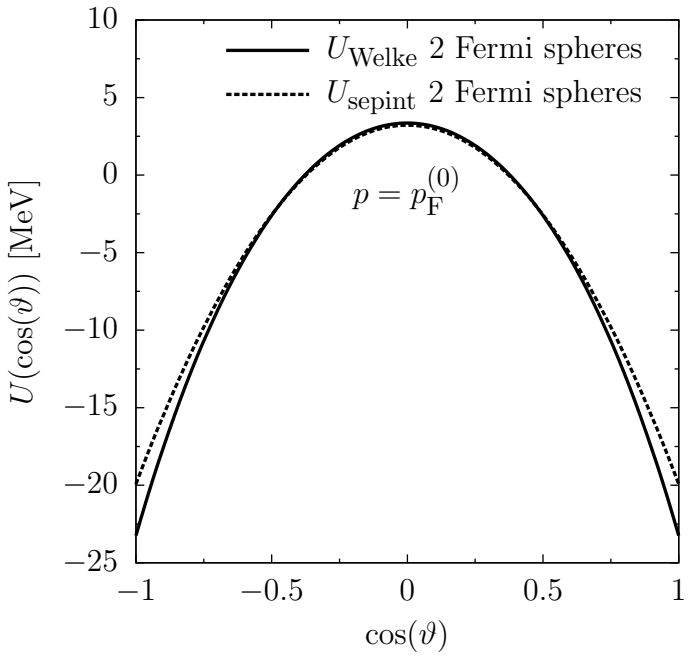

Figure 3.10: Anisotropic mean field U (2.17) in the center of mass of 2 Fermi spheres separated by $p_0 = 800\,\mathrm{MeV}$ as function of $\cos(\vartheta)$ at a momentum magnitude of $p = p_\mathrm{F}^{(0)}$.

The optimal agreement in fig. 3.10 was obtained by tweaking the parameters of our model to $b = 1.19$ and $a = 1.10$. This change leads to some defocussing for the potential energy density in cold nuclear matter and influences the behavior of the anisotropic mean field for the Gaussians. However, the adjustments one needs to make to obtain a reasonable

concordance between Welke and the separable model in fig. 3.10 are satisfyingly small.

3.4 Contribution to the velocity field due to an anisotropic mean field

Before outlining the advantages of our separable model for BUU calculations, compared to Welke, we would like to present an exceptional finding associated with our model. From the mean field U, one can calculate its contribution $\Delta\mathbf{v}$ to the velocity field $\mathbf{v}$ via

$$\Delta\mathbf{v} = \nabla_{\mathbf{p}} U(\mathbf{p}). \tag{3.12}$$

Out of curiosity we did this for $\varepsilon = 0.0$ and $\varepsilon = 1.5$, using a Gaussian phase-space distribution with $\sigma = 150\,\mathrm{MeV}$ at $\rho = 2\rho_0$. The result of the derivative (3.12) is not given here explicitly. We look at the problem for $p_y = 0$. The velocity vectors in the following plots are depicted by arrows, scaled in magnitude by a factor of 200. The underlying Gaussian distribution is indicated by contour lines.

In the isotropic case (cf. fig. 3.11), particle velocities $\Delta\mathbf{v}$ point radially away from the center of mass and follow straight field lines. Suprisingly, for $\varepsilon = 1.5$ (cf. fig. 3.12), field lines are curved and particles try to escape perpendicular to the beam axis. However, compared to the full velocity field

$$\mathbf{v} = \frac{\mathbf{p}}{m} + \nabla_{\mathbf{p}} U(\mathbf{p}), \tag{3.13}$$

this effect is weak for anisotropies ε in the range of interest. Given that the distribution of particles in momentum is anisotropic the findings in fig. 3.12 indicate that the distribution

in velocity is more isotropic. As a consequence of this behavior, we expect a strengthening of the elliptic flow at an early stage of the collision.

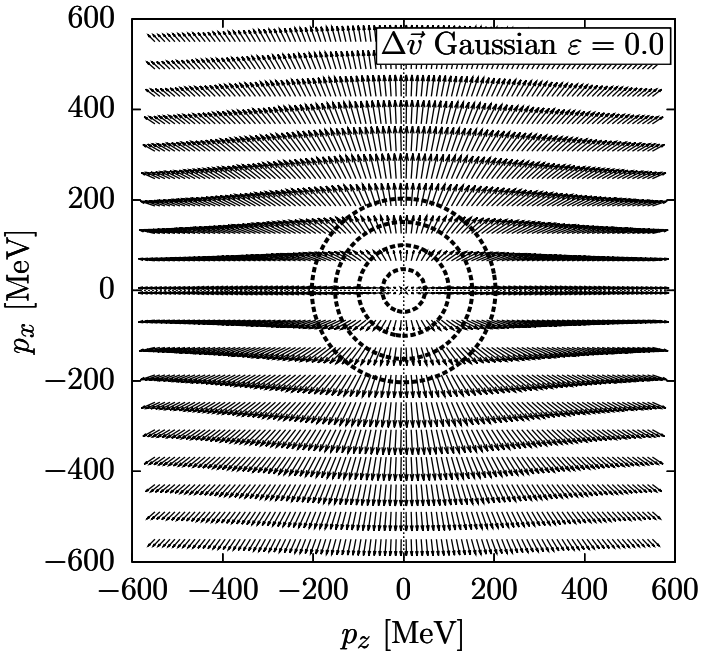

Figure 3.11: Contribution to the velocity field $\Delta\mathbf{v}$ associated with our mean field (2.17) for an isotropic Gaussian ($\varepsilon = 0$) in 2 dimensions.

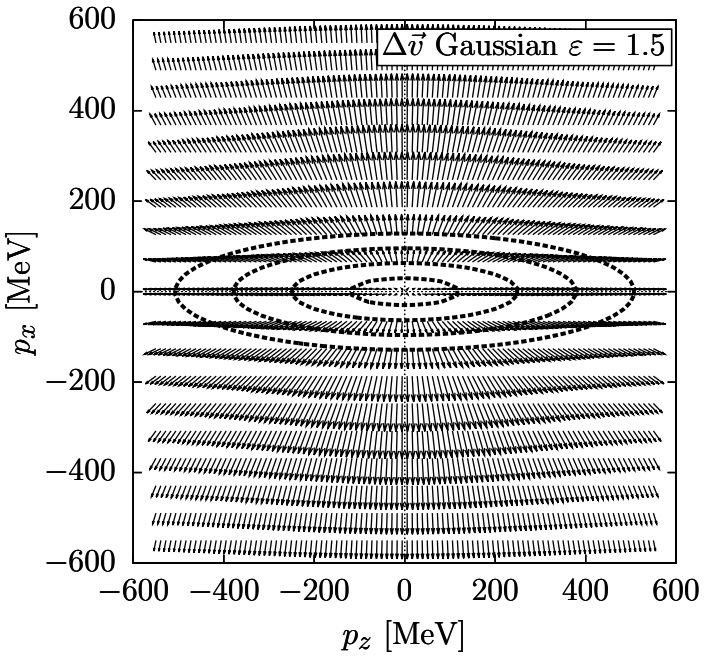

Figure 3.12: Contribution to the velocity field $\Delta\mathbf{v}$ associated with our mean field (2.17) for an anisotropic Gaussian ($\varepsilon = 1.5$) in 2 dimensions.

Chapter 4

Proposed organization of BUU transport simulations

Beyond the scope of this thesis is the actual application of the anisotropic mean field, which we derived in the previous chapters, to reaction simulations, namely BUU calculations. However, in order to stress the relevance of our work, we will provide a brief prescription how to use the model in reactions and name the benefits one gains from using it.

The foundation of BUU is the Boltzmann transport equation [Ber84],[Dan00] for the single-particle distribution function $f(\mathbf{p}, \mathbf{r}, t)$. In order to determine the state of the system one needs to solve the Boltzmann equation for f in every time step t:

$$\frac{\partial f}{\partial t} + \frac{\partial \epsilon}{\partial \mathbf{p}} \frac{\partial f}{\partial \mathbf{r}} - \frac{\partial \epsilon}{\partial \mathbf{r}} \frac{\partial f}{\partial \mathbf{p}} = I_{\text{coll}}(f). \tag{4.1}$$

The collision integral on the r.h.s. of (4.1) accounts for the time evolution of the single-particle phase-space density f evoked by two-body collisions. The mean field U enters the Boltzmann equation on the l.h.s. which takes the motion of particles in the field into account. In order to find the single-particle energies ϵ one has to take the functional derivative of the

system's net energy E with respect to the phase-space density f:

$$\begin{aligned}\epsilon &= \frac{\delta E}{\delta f} \\ &= \frac{p^2}{2m} + \frac{\delta V}{\delta f} \\ &= \frac{p^2}{2m} + U. \end{aligned} \tag{4.2}$$

If the p-dependent part of the mean field is parameterized in terms of an integral

$$U(\mathbf{r}, \mathbf{p}) \propto \int d^3p' \, \frac{f(\mathbf{r}, \mathbf{p}')}{1 + \left[\frac{\mathbf{p}-\mathbf{p}'}{\Lambda}\right]^2}, \tag{4.3}$$

as in the model by Welke *et al.*, one has to determine a different 3-dimensional integral for every momentum $\mathbf{p}$ and position $\mathbf{r}$. The latter is either computationally costly or gives rise to large errors for a low number of Monte Carlo sample points in phase space. In the framework of our model (2.14) one would have to evaluate the integrals in the isotropic term and in T^{zz} per spatial location, once per time step. This is a significant advantage of our model over the parameterization by Welke *et al.*.

Since the primary anisotropy occuring during much of the reaction is a broadened f in beam direction, our model – where a reduction to T^{zz} is intrinsically built-in – naturally qualifies for describing such systems in a cost-effective way.

Chapter 5

Conclusion

In this thesis, we developed a nucleonic mean field U which explicitly exhibits an anisotropic behavior for anisotropic phase-space densities f, and that can significantly reduce computational effort and error-proneness in transport simulations. On that account, we made the nuclear energy functional separable in momentum space in terms of an expansion in spherical harmonics. As reference and guideline during the process of setting up our model, the parameterizations of V and U by Welke *et al.* [Wel88] were used. We step by step evolved the elements of our model by breaking up the original – and in comparison to our parameterization very costly – convolution in the potential energy density, substituting it with scalar and tensorial terms, both symmetric in the single-particle properties, and taking the functional derivative of V with respect to f to obtain U in a simple form. Our model comprises two parameters, one of them – b – mainly relevant in isotropic scenarios, the other one – a – important for characterizing the anisotropy of the mean field. We started the process of modeling by looking at cold nuclear matter properties, also regarding Welke's V and U, and trying to mimic their behavior within our separable framework. Since we obtained a good practical agreement between the models, we proceeded by considering (isotropic) excited matter described by a Gaussian phase-space density. After mapping the Gaussian onto the isotropic ground state by appropriately adjusting its width σ and finding insignificant deviations for the mean field as function of momentum p, we increased the temperature T of the system up to 170 MeV observing growing discrepancies between the models. However,

we showed that by adding another isotropic term to our parameterization of U one can successfully reduce the deviations for high T. We also looked at the potential energy density V for an excited Gaussian state as function of temperature and found a good agreement for the parameter value inferred from cold nuclear matter. In order to constrain the anisotropy immanent in our mean field U, we made the Gaussian distribution anisotropic by introducing the quantity ε and aimed at concordance between Welke and our separable approach when plotting U as a parabolic function of $\cos(\vartheta)$. We found a good agreement between the models especially for strong anisotropies when adjusting a accordingly. Additionally, when considering the energy density V of an anisotropic Gaussian as function of ε, we found that the ε^2-dependence of the tensorial term is insufficient to approximate Welke due to the sign of the ε-parabola's curvature. However, we could describe Welke by using an ϵ-dependent scalar part and the regular Skyrme parameterization for the ρ-dependent part. Presumably, this is related to V being a more integral quantity and U a more differential one. To test our model with a scenario that has been dealt with in the literature we found the 2-Fermi-sphere situation described in [Wel88] appealing since its mean field is highly anisotropic. By portraying the mean field of 2 Fermi spheres approaching each other in momentum space with our anisotropic model we could show that our ansatz is generally applicable even if the shape of the system is not Gaussian. When looking at the contribution $\Delta\mathbf{v}$ to the velocity field $\mathbf{v}$ associated with our mean field parameterization for an isotropic and an anisotropic Gaussian distribution function, we found that particle velocities for a strongly anisotropic scenario of $\varepsilon = 1.5$ tend to be weakly oriented along the perpendicular axis. Consequently, one would expect a strengthening in the experimental observable of elliptic flow. Finally, we discussed the computational benefit of using our model in BUU transport calculations. For these simulations, integrals are commonly evaluated through Monte Carlo. The cost of many

integrals is usually reduced by fewer Monte Carlo sampling points in phase space leading to larger errors. In the framework of our separable model, significantly less integrals need to be evaluated than e.g. in the ansatz by Welke *et al.*, allowing for more accurate Monte Carlo sampling and for accelerated computation. However, we have not yet proceeded to an actual implementation due to the limited scope of this thesis.

To conclude, we presented a simple, user-friendly way of describing the potential energy density V and the mean field U, associated with momentum p, in heavy-ion collisions. Our model is especially powerful in terms of dealing with strongly anisotropic scenarios and with respect to its applicability in transport simulations.

BIBLIOGRAPHY

BIBLIOGRAPHY

[Aic87] J. Aichelin *et al.*, Phys. Rev. Lett. **58**, 1926 (1987)

[App89] J. Applequist, J. Phys. **A**: Math. Gen. **22**, 4303 (1989)

[Ber84] G.F. Bertsch, H. Kruse and S. Das Gupta, Phys. Rev. **C 29**, 673 (1984)

[Bla76] J.P. Blaizot, D. Gogny and B. Grammaticos, Nucl. Phys. **A 265**, 315 (1976)

[Dan00] P. Danielewicz, Nucl. Phys. **A 673**, 375 (2000)

[Dan05] P. Danielewicz and S. Pratt, Phys. Lett. **B 618**, 60 (2005)

[Gal87] C. Gale, G.F. Bertsch and S. Das Gupta, Phys. Rev. **C 35**, 1666 (1987)

[Gog75] D. Gogny, in *Nuclear Self Consistent Fields*, edited by G. Ripka and M. Porneuf, p. 333 (North-Holland, Amsterdam, 1975)

[Noz99] P. Nozieres and D. Pines, *The Theory Of Quantum Liquids*, (Westview Press, 1999)

[Pan93] Q. Pan and P. Danielewicz, Phys. Rev. Lett. **70**, 2062 (1993)

[Sky59] T.H.R. Skyrme, Nucl. Phys. **9**, 615 (1959)

[Tei97] S. Teis *et al.*, Z. Phys. **A 356**, 421 (1997)

[Ueh33] E.A. Uehling and G.E. Uhlenbeck, Phys. Rev. **43**, 552 (1933)

[Wel88] G.M. Welke *et al.*, Phys. Rev. **C 38**, 2101 (1988)

[Zha94] J. Zhang, S. Das Gupta and C. Gale, Phys. Rev. **C 50**, 1617 (1994)